

M. Cermeño

Evidence for  
DM and its  
detection

Circular  
polarisation of  
photons from  
BSM  
interactions

Circular  
polarised  
signals from  
the GC  
(this work)

Conclusions

# Circular polarisation of gamma rays as a probe of DM-CR electron interactions

Marina Cermeño Gavilán

Centre for Cosmology, Particle Physics and Phenomenology (CP3),  
Université Catholique de Louvain, Belgium.

arXiv: 2103.14658

In collaboration with C. Degrande and L. Mantani

July 28, 2021



# Evidence for dark matter (DM)

M. Cermeño

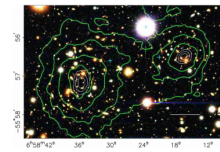
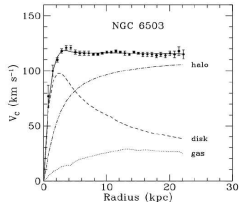
Evidence for  
DM and its  
detection

Circular  
polarisation of  
photons from  
BSM  
interactions

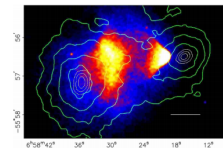
Circular  
polarised  
signals from  
the GC  
(this work)

Conclusions

- Astrophysical (rotation curves, gravitational lenses, cluster dynamics) and cosmological (CMB analysis, structure formation simulations) observations

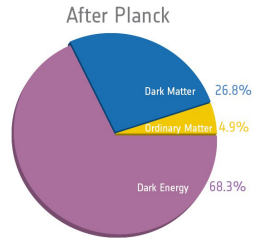


Begeman et al., MNRAS 249 (1991) 523  
Clowe et al., ApJ 648 (2006) L109



- DM density is inferred from data by the Planck Collaboration  
 $\Omega_{CDM} h^2 = 0.120 \pm 0.001$ ,  
 $\Omega_m h^2 = 0.1430 \pm 0.0011$

Planck Collaboration A&A, 641 (2020) A6



# DM distribution in the Galaxy

M. Cermeño

Evidence for  
DM and its  
detection

Circular  
polarisation of  
photons from  
BSM  
interactions

Circular  
polarised  
signals from  
the GC  
(this work)

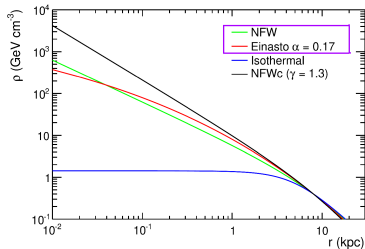
Conclusions

- Well-motivated DM density profiles in our galaxy by the study of rotation curves and N-body simulations

*Einasto, Trudy Inst. Astrofiz. Alma-Ata 5 (1965) 87, NFW, ApJ 462 (1996) 563, Navarro et al., MNRAS 402 (2010) 21, Ludlow, Angulo MNRAS 465 (2017) L84*

$$\rho_{\text{NFW}}(r) = \rho_s \frac{r_s}{r} \left(1 + \frac{r}{r_s}\right)^2$$
$$\rho_{\text{Ein}}(r) = \rho_s \exp\left\{-\frac{2}{\alpha} \left[\left(\frac{r}{r_s}\right)^\alpha - 1\right]\right\}$$

Profiles	Einasto	NFW
$\rho_s$ ( $\text{GeV cm}^{-3}$ )	0.079	0.307
$r_s$ (kpc)	20.0	21.0
$\alpha_s$	0.17	/



*The Fermi-LAT Collaboration PRD 91 (2015) 122002*

- The local DM density  $\rho_{\chi,0} = 0.385 \pm 0.027 \text{ GeV/cm}^3$  at  $r_\odot = 8.5 \text{ kpc}$  from the Galactic Center (GC)

*Catena and Ullio JCAP08 (2010) 004*

# Indirect DM detection

M. Cermeño

Evidence for  
DM and its  
detection

Circular  
polarisation of  
photons from  
BSM  
interactions

Circular  
polarised  
signals from  
the GC  
(this work)

Conclusions

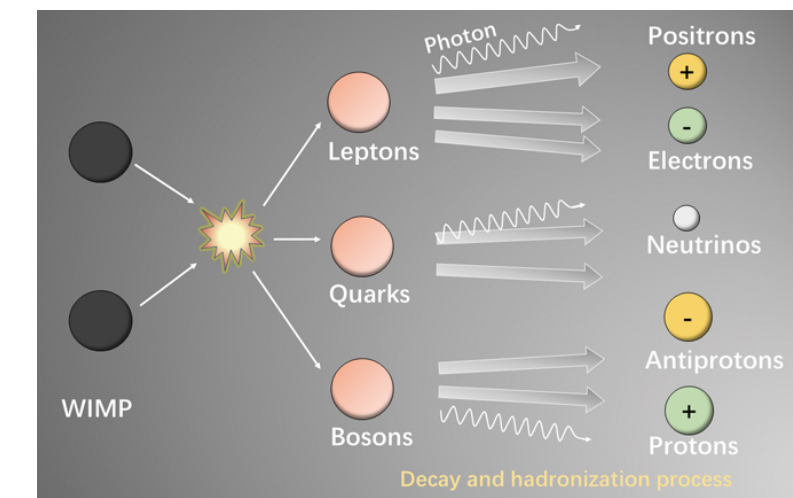


Image by GAO Linqing and LIN Sujie

# Indirect detection: Photon searches

M. Cermeño

Evidence for  
DM and its  
detection

Circular  
polarisation of  
photons from  
BSM  
interactions

Circular  
polarised  
signals from  
the GC  
(this work)

Conclusions

$$\frac{d\Phi}{dE_\gamma}(E_\gamma, \Delta\Omega) = \frac{\langle\sigma v\rangle}{8\pi m_\chi^2} \frac{dN}{dE_\gamma}(E_\gamma) \int_{\Delta\Omega_{\text{obs}}} d\Omega \int_{\text{l.o.s}} ds \rho^2(r(s, \theta))$$

- $\langle\sigma v\rangle$  averaged annihilation cross section of DM particles of mass  $m_\chi$
- $\frac{dN}{dE_\gamma}(E_\gamma)$  energy spectrum per annihilation event
- $\rho(r)$  DM density profile,  $r^2 = s^2 + r_0^2 - 2r_0 s \cos\theta$ ,  $r_0$  radial distance from the observer to the target

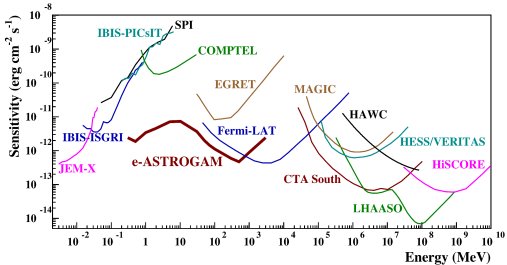


Figure from Tatischeff et al. arXiv:1805.06435

# Circular polarised photons from BSM interactions

M. Cermeño

Evidence for  
DM and its  
detection

Circular  
polarisation of  
photons from  
BSM  
interactions

Circular  
polarised  
signals from  
the GC  
(this work)

Conclusions

- DM can generate circular polarised signals in X-rays or gamma-rays through decays and interactions with SM particles

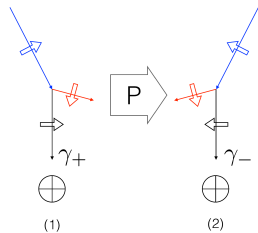
*Kumar et al., PRD 94 (2016) 015022, Elagin et al., PRD 96 (2017) 096008, Bonivento et al., PLB 765 (2017) 127, Boehm et al., JCAP 05 (2017) 043, Huang, Ng, and Yuan, PLB 800 (2020) 135104*

- A net circular polarisation signal is generated when there is an excess of one photon polarisation state over the other
- Parity must be violated in at least one of the dominant photon emission processes

$$\mathcal{A}_- \neq \mathcal{A}_+$$

$$\mathcal{A}_\pm = \sum_{spins} |\epsilon_\pm^\mu \mathcal{M}_\mu|^2$$

$$\epsilon_\pm^\mu(k) = \frac{1}{2}(\mp \epsilon_1^\mu(k) - i \epsilon_2^\mu(k))$$



*Boehm et al., JCAP 05 (2017) 043*

- There must be an asymmetry in the number density of one of the particles in the initial state or CP must be violated

# Circular polarised photon flux from the GC

M. Cermeño

Evidence for  
DM and its  
detection

Circular  
polarisation of  
photons from  
BSM  
interactions

Circular  
polarised  
signals from  
the GC  
(this work)

Conclusions

The flux of circularly polarised photons from  $e^-\tilde{\chi} \rightarrow e^-\tilde{\chi} \gamma_\pm$  at a distance  $r_\odot$

$$\frac{d\Phi_{e\chi,pol}}{dE_\gamma} = \frac{\bar{J}(\Delta\Omega)}{m_{\tilde{\chi}}} \int dE_e \frac{d\phi}{dE_e} \left| \frac{d\sigma_+}{dE_\gamma}(E_e, E_\gamma) - \frac{d\sigma_-}{dE_\gamma}(E_e, E_\gamma) \right|$$

- $\bar{J}(\Delta\Omega) = \frac{1}{\Delta\Omega_{\text{obs}}} \int_{\Delta\Omega_{\text{obs}}} d\Omega \int_{\text{l.o.s}} ds \rho(r(s, \theta)) f(r(s, \theta))$

$f(r) = e^{-\frac{(r-r_\odot)}{r_0}}$  the spatial distribution of CR electrons,  $r_0 = 4$  kpc

*Strong et al., A&A, 422 (2004) L47*

$\rho(r(s, \theta))$  the DM density profile

- $\frac{d\phi}{dE_e}$  the CR electron energy spectrum in units of  $\text{GeV}^{-1} \text{cm}^{-2} \text{s}^{-1} \text{sr}^{-1}$
- $\frac{d\sigma_\pm}{dE_\gamma}(E_e, E_\gamma)$  the differential cross section for  $e^-\tilde{\chi} \rightarrow e^-\tilde{\chi} \gamma_\pm$ , with  $E_e$  the incoming electron energy,  $m_{\tilde{\chi}}$  the DM mass and  $E_\gamma$  the photon energy.

# The model

M. Cermeño

Evidence for  
DM and its  
detection

Circular  
polarisation of  
photons from  
BSM  
interactions

Circular  
polarised  
signals from  
the GC  
(this work)

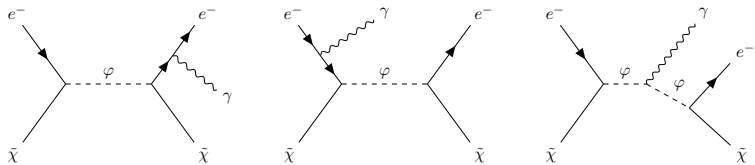
Conclusions

$$\mathcal{L}_{DM} = i\bar{\psi}_{\tilde{\chi}}(\not{D} - m_{\tilde{\chi}})\psi_{\tilde{\chi}} + D_\mu \varphi^\dagger D^\mu \varphi - m_\varphi \varphi^\dagger \varphi + (a_R \bar{e}_R \psi_{\tilde{\chi}} \varphi + h.c.).$$

[Bringmann et al., JCAP 07 \(2012\) 054](#), [Garny et al., JCAP 12 \(2013\) 640](#), [Kopp, Michaels, Smirnov, JCAP 04 \(2014\) 022](#), [Okada, Toma, PLB 750 \(2015\) 266](#), [Garny, Ibarra, Vogl, Int.J.Mod.Phys.D 24 \(2015\) 07, 1530019](#)

$\tilde{\chi}$  Majorana fermion,  $\varphi$  charged scalar mediator,  $e_R$  right-handed electrons

- $m_\varphi \gtrsim m_{\tilde{\chi}}$
- $\Delta M = m_\varphi - m_{\tilde{\chi}} \ll m_\varphi \Rightarrow$  resonantly enhanced 2 to 3 radiative processes provide a peak in the spectrum



# CR electron energy spectrum

M. Cermeño

Evidence for  
DM and its  
detection

Circular  
polarisation of  
photons from  
BSM  
interactions

Circular  
polarised  
signals from  
the GC  
(this work)

Conclusions

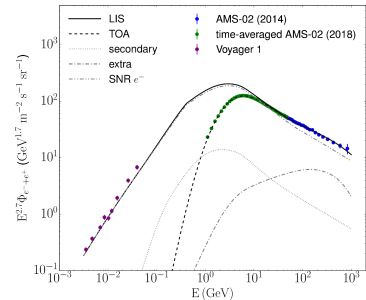
## The local interstellar spectrum (LIS)

$$\begin{aligned} E_e^{-1.2} & \text{ for } E_e < 0.05 \text{ GeV}, \\ E_e^{-2} & \text{ for } 0.05 \text{ GeV} \lesssim E_e \lesssim 4 \text{ GeV}, \\ E_e^{-3} & \text{ for } E_e > 4 \text{ GeV}. \end{aligned}$$

## Injected spectrum

$$\frac{d\Phi_{\text{inj}}}{dE_e} = \begin{cases} k_{e,\text{inj}} \left( \frac{E_e}{\text{GeV}} \right)^{-2.13} & \text{for } E_e \leq 0.109 \text{ GeV} \\ \frac{k_{e,\text{inj}}}{8.9 \cdot 10^{-3}} \left( \frac{E_e}{0.109 \text{ GeV}} \right)^{-2.57} & \text{for } E_e > 0.109 \text{ GeV} \end{cases}$$

with  $k_{e,\text{inj}} = 6.98 \cdot 10^{-3} \text{ GeV}^{-1} \text{ cm}^{-2} \text{ s}^{-1} \text{ sr}^{-1}$ .



Vittino et al., PRD 100 (2019) 043007

# Results: Photon flux and circular polarisation

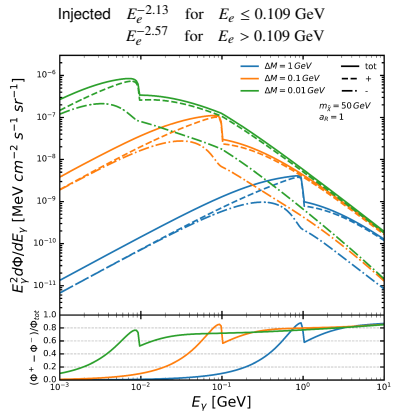
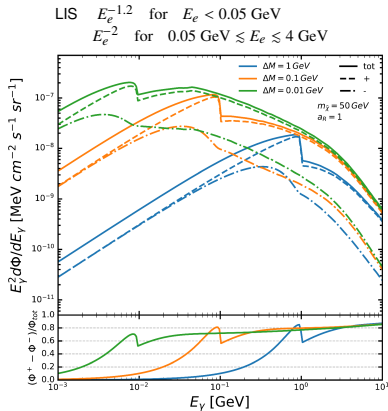
M. Cermeño

Evidence for  
DM and its  
detection

Circular  
polarisation of  
photons from  
BSM  
interactions

Circular  
polarised  
signals from  
the GC  
(this work)

Conclusions



$$\frac{\Phi^+ - \Phi^-}{\Phi_{tot}} \equiv \frac{\frac{d\Phi_{e\tilde{\chi}, pol}}{dE_\gamma}}{\frac{d\Phi_{e\tilde{\chi}}}{dE_\gamma}}, \quad \frac{d\Phi_{e\tilde{\chi}, pol}}{dE_\gamma} = \frac{d\Phi_{e\tilde{\chi}, +}}{dE_\gamma} - \frac{d\Phi_{e\tilde{\chi}, -}}{dE_\gamma}$$

Asymmetries up to 90 %

# Results: Photon flux and circular polarisation

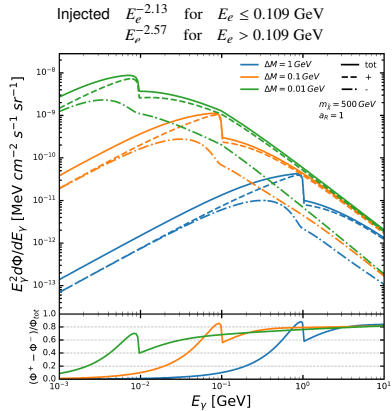
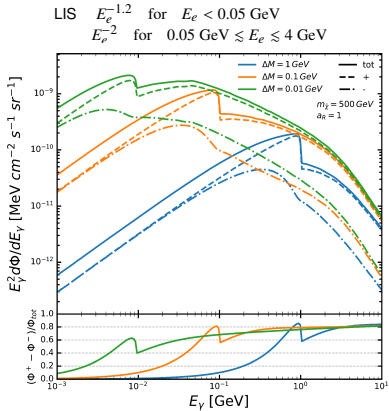
M. Cermeño

Evidence for  
DM and its  
detection

Circular  
polarisation of  
photons from  
BSM  
interactions

Circular  
polarised  
signals from  
the GC  
(this work)

Conclusions



$$\frac{\Phi^+ - \Phi^-}{\Phi_{\text{tot}}} \equiv \frac{\frac{d\Phi_{e\tilde{\chi},\text{pol}}}{dE_\gamma}}{\frac{d\Phi_{e\tilde{\chi}}}{dE_\gamma}}, \quad \frac{d\Phi_{e\tilde{\chi},\text{pol}}}{dE_\gamma} = \frac{d\Phi_{e\tilde{\chi},+}}{dE_\gamma} - \frac{d\Phi_{e\tilde{\chi},-}}{dE_\gamma}$$

Asymmetries up to 90 %

Flux scales as  $\sim \frac{1}{m_{\tilde{\chi}}^2}$

# Results: Photon flux and circular polarisation

M. Cermeño

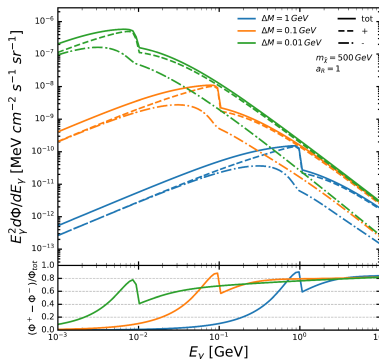
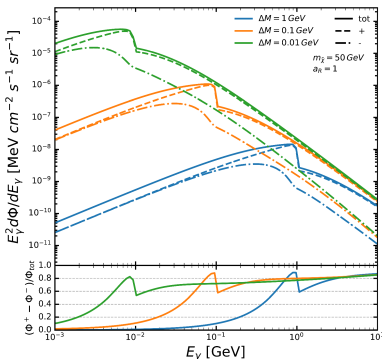
Evidence for  
DM and its  
detection

Circular  
polarisation of  
photons from  
BSM  
interactions

Circular  
polarised  
signals from  
the GC  
(this work)

Conclusions

- Energy spectrum  $\frac{d\Phi}{dE_e} = k_e \left( \frac{E_e}{\text{GeV}} \right)^{-3}$ ,  $k_e = 10^{-2} \text{ GeV}^{-1} \text{ cm}^{-2} \text{ s}^{-1} \text{ sr}^{-1}$



- The electron energy spectrum has a relevant impact on the final results
- Higher circular polarised fluxes could be obtain close to cosmic accelerators (AGNs, pulsars, SNRs...) ⇒ Work in progress

# Prospects of detection

M. Cermeño

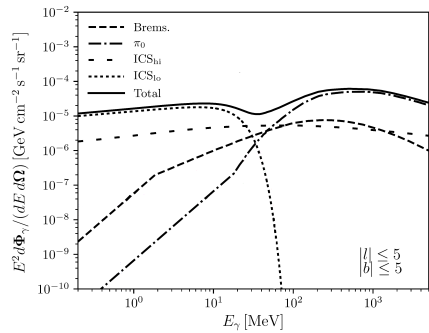
Evidence for  
DM and its  
detection

Circular  
polarisation of  
photons from  
BSM  
interactions

Circular  
polarised  
signals from  
the GC  
(this work)

Conclusions

- Standard circular polarisation: synchrotron emission and curvature radiation
- Gamma-rays from the GC: ICS, bremsstrahlung and inelastic collisions of high energy CRs with the ambient medium
- No important circular polarisation fraction expected in gamma-rays



Adapted from  
[Bartels, Gaggero, Weniger, JCAP05 \(2017\) 001](#)

- $\frac{N_{\text{signal}}}{\sqrt{N_{\text{back}}}} \sim 3 \Rightarrow E_\gamma^2 \frac{d\Phi_{e\chi}}{dE_\gamma} \sim 10^{-5} \text{ MeV cm}^{-2} \text{ s}^{-1} \text{ sr}^{-1}$ ,  $\Delta t \sim 10^8 \text{ s}$  (e-ASTROGAM)
- Detectable fluxes for  $m_\chi \sim 5 \text{ GeV}$ , but  $m_\chi \sim m_\varphi > M_Z/2 = 45 \text{ GeV}$
- Exploit the polarisation fractions to increase the sensitivity to the signal

# Conclusions

M. Cermeño

Evidence for  
DM and its  
detection

Circular  
polarisation of  
photons from  
BSM  
interactions

Circular  
polarised  
signals from  
the GC  
(this work)

Conclusions

- We have calculated for the first time the flux of circular polarised photons coming from the GC due to a P violating interaction between DM and CR electrons
- Our fluxes can reach a circular polarisation asymmetry of 90 %
- The signal obtained is not detectable unless a new technique which exploits the circular polarisation fraction is used or UV assumptions are made concerning a full gauge invariant theory to evade  $m_\varphi \leq 45$  GeV
- Both the fraction of circular polarisation and the flux of photons are highly dependent on the mass splitting and the electron energy spectrum
- A different P violating model or source could increase the intensity of the flux allowing e-ASTROGAM to detect these signals and encouraging to exploit the polarisation fraction as a characterisation feature

M. Cermeño

Evidence for  
DM and its  
detection

Circular  
polarisation of  
photons from  
BSM  
interactions

Circular  
polarised  
signals from  
the GC  
(this work)

Conclusions

# Backup slides

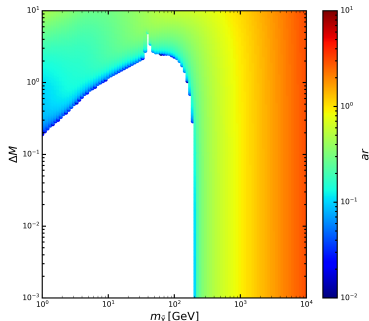
# Relic density

- Assuming a thermal production of DM

$$\Omega_\chi h^2 \sim \frac{1}{\sigma v_{eff}}, \quad \sigma v_{eff} = \sigma v_{\tilde{\chi}\tilde{\chi}} + \sigma v_{\tilde{\chi}\varphi} e^{-\frac{\Delta M}{T}} + \sigma v_{\varphi\varphi} e^{-\frac{2\Delta M}{T}},$$

$\sigma v_{\tilde{\chi}\tilde{\chi}} \sim \frac{a_R^4}{m_\chi^2}$ ,  $\sigma v_{\tilde{\chi}\varphi} \sim \frac{a_R^2 g^2}{m_\chi^2}$ ,  $\sigma v_{\varphi\varphi} \sim \frac{g^4}{m_\chi^2}$ , where  $g$  is a gauge coupling

- For each point  $(m_{\tilde{\chi}}, \Delta M) \Rightarrow a_R$  that yields  $\Omega_\chi h^2 = 0.120 \pm 0.001$



M. Cermeño

Evidence for  
DM and its  
detection

Circular  
polarisation of  
photons from  
BSM  
interactions

Circular  
polarised  
signals from  
the GC  
(this work)

Conclusions

# Indirect detection constraints

M. Cermeño

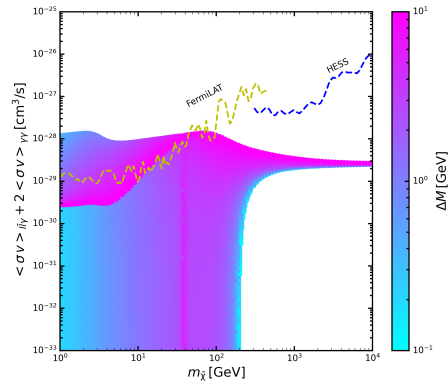
Evidence for  
DM and its  
detection

Circular  
polarisation of  
photons from  
BSM  
interactions

Circular  
polarised  
signals from  
the GC  
(this work)

Conclusions

- $\tilde{\chi}\tilde{\chi} \rightarrow e^+e^-$  velocity suppressed
  - $\tilde{\chi}\tilde{\chi} \rightarrow e^-e^+\gamma$  and  $\tilde{\chi}\tilde{\chi} \rightarrow \gamma\gamma$  relevant channels
  - yellow and blue lines are the upper limits from Fermi-LAT and HESS
- Ackermann et al., PRD 727 D 91 (2015) 122002,*  
*Abdallah et al., PRL 731120 (2018) 201101*
- For  $m_\chi \gtrsim 200$  GeV cases with  $\Delta M < 10^{-1}$  GeV overlap with the rest of the solutions



# Collider constraints

M. Cermeño

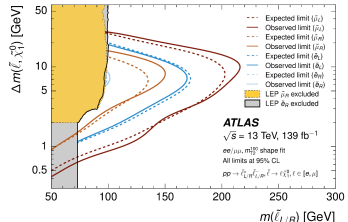
Evidence for  
DM and its  
detection

Circular  
polarisation of  
photons from  
BSM  
interactions

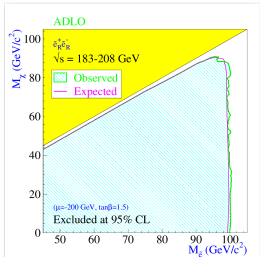
Circular  
polarised  
signals from  
the GC  
(this work)

Conclusions

- $\varphi$  can be pair produced through EW interactions
  - Constraints from  $\varphi \rightarrow \tilde{\chi} e^-$ , unless  $\Delta M$  is too small
  - LHC excludes only  $m_\varphi \lesssim 100$  GeV for  $\Delta M \sim$  few GeV
  - LEP constraints evaded  $\frac{m_\varphi}{m_\chi} \leq 1.03$
  - Constraints from mono-photon events at LEP less stringent than the ones from Fermi LAT and HESS
- Kopp, Michaels, Smirnov, JCAP 04 (2014) 022*
- Strongest constraint  $\Rightarrow Z$  width,  $m_\varphi > M_Z/2 = 45$  GeV



Aad et al., PRD 101 (2020) 052005



LEP2 SUSY Working Group (2004)

# Direct detection constraints

M. Cermeño

Evidence for  
DM and its  
detection

Circular  
polarisation of  
photons from  
BSM  
interactions

Circular  
polarised  
signals from  
the GC  
(this work)

Conclusions

$$\mathcal{L}_{eff} = \mathcal{A} \bar{\psi}_{\tilde{\chi}} \gamma^\mu \gamma^5 \psi_{\tilde{\chi}} \partial^\nu F_{\mu\nu}$$

$\mathcal{A}$  the anapole form factor

- Upper bounds by XENON1T (solid) and the projected LZ (dashed)

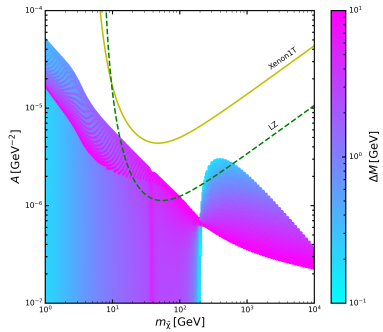
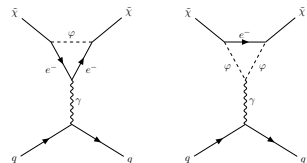
Aprile et al., PRL 121 (2018) 111302,

Mount et al., arXiv:1703.09144

- Points with  $\frac{m_\varphi^2}{m_{\tilde{\chi}}^2} < 1.001$  not shown, perturbative approach used to obtain  $\mathcal{A}$  is not valid, need for the next term in the expansion

Kopp, Michaels, Smirnov, JCAP 04 (2014) 022,

Baker, Thamm, JHEP 10 (2018) 187



# Anapole form factor

M. Cermeño

Evidence for  
DM and its  
detection

Circular  
polarisation of  
photons from  
BSM  
interactions

Circular  
polarised  
signals from  
the GC  
(this work)

Conclusions

Our Majorana DM particle can interact via one loop anapole moment

$$\mathcal{L}_{eff} = \mathcal{A} \bar{\psi}_{\tilde{\chi}} \gamma^\mu \gamma^5 \psi_{\tilde{\chi}} \partial^\nu F_{\mu\nu}.$$

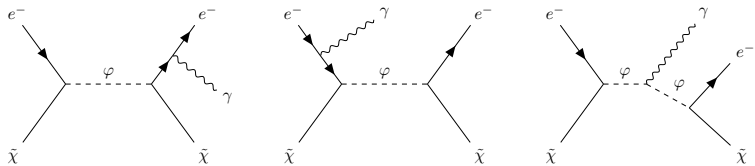
The anapole form factor for  $|q^2| \ll m_e^2$

$$\mathcal{A} = -\frac{ea_R^2}{32\pi^2 m_{\tilde{\chi}}^2} \left[ \frac{-10 + 12 \log\left(\frac{\sqrt{|q^2|}}{m_{\tilde{\chi}}}\right) - (3 + 9r^2) \log(r^2 - 1) - (3 - 9r^2) \log r^2}{9(r^2 - 1)} \right]$$

Kopp, Michaels, Smirnov, JCAP 04 (2014) 022, Baker, Thamm, JHEP 10 (2018) 187

- $\sqrt{|q^2|} = \sqrt{2E_r m_T}$  the transferred momentum, where  $E_r \sim \frac{1}{2} m_{\tilde{\chi}} v_{\tilde{\chi}}^2$  is the recoil energy and  $m_T$  the mass of the target of the experiment
- $r = \frac{m_\varphi}{m_{\tilde{\chi}}}$ , for  $r^2 \lesssim 1.001$  the perturbation theory is not valid anymore, need of the next term in the expansion

# Resonances of the process



$p_{\tilde{\chi}} = (m_{\tilde{\chi}}, \vec{0})$ ,  $p_e = (E_e, \vec{p}_e)$  the incoming DM and electron four-momenta,  
 $p'_{\tilde{\chi}} = (E'_{\tilde{\chi}}, \vec{p}'_{\tilde{\chi}})$ ,  $p'_e = (E'_e, \vec{p}'_e)$  the outgoing ones

## ■ Two resonances

$$s = (p_e + p_{\tilde{\chi}})^2 = m_{\varphi}^2 \Rightarrow E_{R1} = \frac{m_{\varphi}^2 - m_{\tilde{\chi}}^2}{2m_{\tilde{\chi}}} \approx \Delta M$$

$$s' = (p'_e + p'_{\tilde{\chi}})^2 = m_{\varphi}^2 \Rightarrow E_{R2} = \frac{m_{\varphi}^2 - m_{\tilde{\chi}}^2 + 2m_{\tilde{\chi}}E_{\gamma}}{2(m_{\tilde{\chi}} - E_{\gamma}(1 - \cos \theta_{\gamma}))}$$

with  $\theta_{\gamma}$  the angle between the emitted photon and the incoming CR electron

# Resonances of the process

M. Cermeño

Evidence for  
DM and its  
detection

Circular  
polarisation of  
photons from  
BSM  
interactions

Circular  
polarised  
signals from  
the GC  
(this work)

Conclusions

When the minimum electron energy

$$E_{\min} = \frac{E_\gamma}{1 - \frac{E_\gamma}{m_{\tilde{\chi}}} \cos \theta_\gamma}$$

is higher than  $E_{R1}$ ,

$$E_\gamma > \frac{m_{\tilde{\chi}}(m_\varphi^2 - m_{\tilde{\chi}}^2)}{2m_{\tilde{\chi}}^2 + (m_\varphi^2 - m_{\tilde{\chi}}^2)(1 - \cos \theta_\gamma)}$$

the first resonance cannot happen anymore.

The drop-off between  $E_{\gamma,1} = \frac{m_{\tilde{\chi}}(m_\varphi^2 - m_{\tilde{\chi}}^2)}{2m_\varphi^2}$  and  $E_{\gamma,2} = \frac{(m_\varphi^2 - m_{\tilde{\chi}}^2)}{2m_{\tilde{\chi}}}$ .

For  $\Delta M \ll m_\varphi \sim m_{\tilde{\chi}} \Rightarrow E_{\gamma,1} \sim E_{\gamma,2} \sim \Delta M$ .

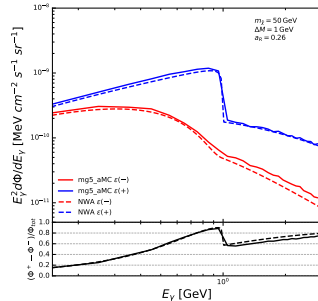
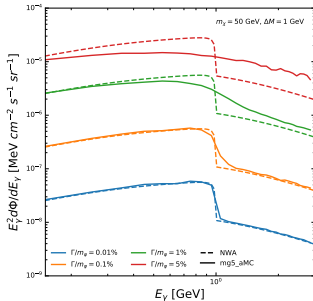
Beyond this energy, only the second resonance contributes to the flux.

# The Narrow Width Approximation

- We are interested in cases with  $\Delta M \ll m_\varphi$
- the total width of the mediator is

$$\Gamma_{\text{tot}} \sim \Gamma_{\varphi \rightarrow e^- \tilde{\chi}} = \frac{1}{8\pi} a_R^2 \frac{(m_\varphi^2 - m_{\tilde{\chi}}^2)^2}{2m_\varphi^3} \approx \frac{1}{4\pi} a_R^2 \frac{(\Delta M)^2}{m_\varphi}$$

- $\frac{\Gamma_{\text{tot}}}{m_\varphi} \propto \left( \frac{\Delta M}{m_\varphi} \right)^2 \ll 1 \Rightarrow \text{NWA}$



M. Cermeño

Evidence for  
DM and its  
detection

Circular  
polarisation of  
photons from  
BSM  
interactions

Circular  
polarised  
signals from  
the GC  
(this work)

Conclusions

# The Narrow Width Approximation

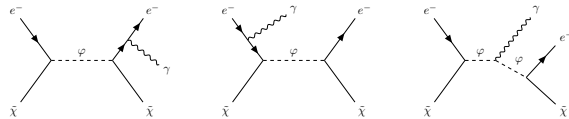
M. Cermeño

Evidence for  
DM and its  
detection

Circular  
polarisation of  
photons from  
BSM  
interactions

Circular  
polarised  
signals from  
the GC  
(this work)

Conclusions



$$\frac{d\tilde{\Phi}_{e\tilde{\chi},\pm}}{dE_\gamma} \equiv \frac{m_{\tilde{\chi}}}{J} \frac{d\Phi_{e\tilde{\chi},\pm}}{dE_\gamma} = \int dE_e \frac{d\phi}{dE_e} \frac{d\sigma_\pm}{dE_\gamma}(E_e, E_\gamma),$$

$$\frac{d\tilde{\Phi}_{e\tilde{\chi},\pm}}{dE_\gamma} = \int \frac{d\phi}{dE_e} \frac{d\tilde{\sigma}_{1\pm}}{dE_\gamma} dE_e + \int \frac{d\phi}{dE_e} \frac{d\tilde{\sigma}_{2\pm}}{dE_\gamma} dE_e,$$

the differential cross section for the first diagram

$$\frac{d\tilde{\sigma}_{1\pm}}{dE_\gamma} = \sigma_{e-\tilde{\chi} \rightarrow \varphi}(E_e) \frac{d\Gamma_{\varphi \rightarrow e^-\tilde{\chi}\gamma^\pm}}{dE_\gamma}(E_\gamma) \frac{1}{\Gamma_{\text{tot}}}$$

the differential cross section for the other two

$$\frac{d\tilde{\sigma}_{2\pm}}{dE_\gamma} = \frac{d\sigma_{e-\tilde{\chi} \rightarrow \varphi\gamma^\pm}}{dE_\gamma}(E_e, E_\gamma) \frac{\Gamma_{\varphi \rightarrow e^-\tilde{\chi}}}{\Gamma_{\text{tot}}}$$

with  $\Gamma_{\text{tot}} = \Gamma_{\varphi \rightarrow e^-\tilde{\chi}} + \Gamma_{\varphi \rightarrow e^-\tilde{\chi}\gamma^\pm}$

# Impact of the first resonance on the asymmetry

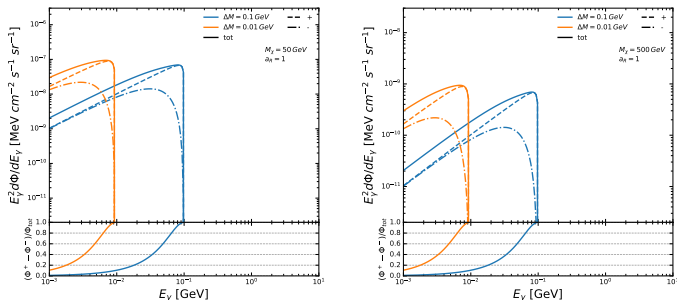
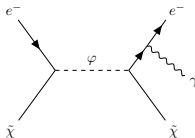
M. Cermeño

Evidence for  
DM and its  
detection

Circular  
polarisation of  
photons from  
BSM  
interactions

Circular  
polarised  
signals from  
the GC  
(this work)

Conclusions



LIS spectrum

# Impact of the second resonance on the asymmetry

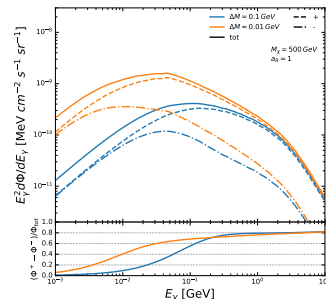
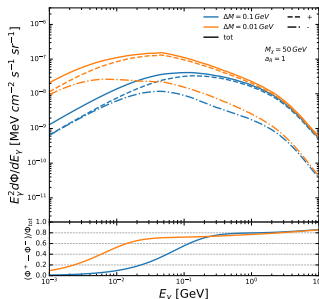
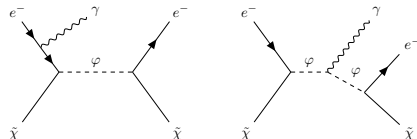
M. Cermeño

Evidence for  
DM and its  
detection

Circular  
polarisation of  
photons from  
BSM  
interactions

Circular  
polarised  
signals from  
the GC  
(this work)

Conclusions



LIS spectrum

# CR electron energy spectrum

M. Cermeño

Evidence for  
DM and its  
detection

Circular  
polarisation of  
photons from  
BSM  
interactions

Circular  
polarised  
signals from  
the GC  
(this work)

Conclusions

The local interstellar spectrum (LIS)

$$E_e^{-1.2} \quad \text{for } E_e < 0.05 \text{ GeV},$$

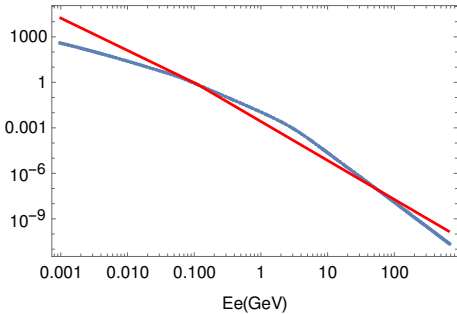
$$E_e^{-2} \quad \text{for } 0.05 \text{ GeV} \lesssim E_e \lesssim 4 \text{ GeV},$$

$$E_e^{-3} \quad \text{for } E_e > 4 \text{ GeV}.$$

Injected spectrum

$$\frac{d\Phi_{\text{inj}}}{dE_e} = \begin{cases} k_{e,\text{inj}} \left( \frac{E_e}{\text{GeV}} \right)^{-2.13} & \text{for } E_e \leq 0.109 \text{ GeV} \\ \frac{k_{e,\text{inj}}}{8.9 \cdot 10^{-3}} \left( \frac{E_e}{0.109 \text{ GeV}} \right)^{-2.57} & \text{for } E_e > 0.109 \text{ GeV} \end{cases}$$

$$\frac{d\phi}{dE_e} \left( \frac{1}{\text{GeV cm}^2 \text{ sr s}} \right)$$



# CR electron energy spectrum

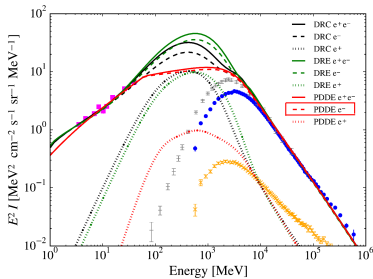
M. Cermeño

Evidence for  
DM and its  
detection

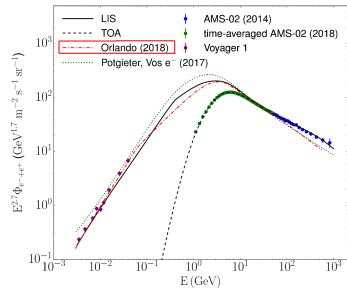
Circular  
polarisation of  
photons from  
BSM  
interactions

Circular  
polarised  
signals from  
the GC  
(this work)

Conclusions



Orlando, MNRAS 475 (2018) 2724



Vittino et al., PRD 100 (2019) 043007

# Results: Photon flux and circular polarisation

M. Cermeño

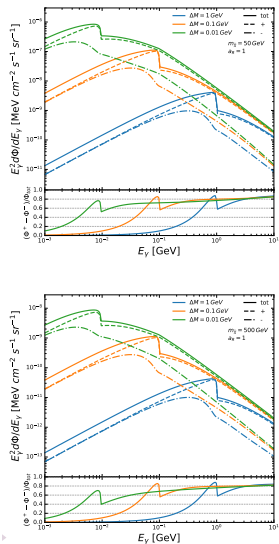
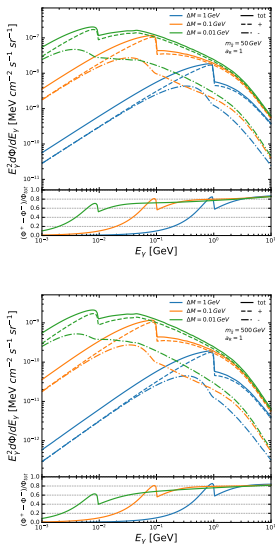
Evidence for  
DM and its  
detection

Circular  
polarisation of  
photons from  
BSM  
interactions

Circular  
polarised  
signals from  
the GC  
(this work)

Conclusions

- Left: LIS
- Right: injected spectrum
- Einasto profile,  
 $\frac{\bar{J}_{\text{NFW}}}{\bar{J}_{\text{Ein}}} \sim 0.7$
- Thermal relic DM,  
rescale flux by  $a_R^2$
- $m_{\tilde{\chi}} = 50$  GeV  
underabundant
- Dirac DM, rescale  
flux by  $\frac{\rho_{\tilde{\chi}}}{\rho_{\chi} + \rho_{\tilde{\chi}}}$
- $m_\phi \geq 45$  GeV cannot  
be easily evaded



# Scattering vs annihilation

M. Cermeño

Evidence for  
DM and its  
detection

Circular  
polarisation of  
photons from  
BSM  
interactions

Circular  
polarised  
signals from  
the GC  
(this work)

Conclusions

## The annihilation rate

$$q_{\tilde{\chi}\tilde{\chi}} \sim \langle \sigma v \rangle \frac{\rho_0}{m_{\tilde{\chi}}} \sim \frac{a_R^4 e^2}{(4\pi)^2 m_{\tilde{\chi}}^2} v_{\tilde{\chi}} \frac{\rho_0}{m_{\tilde{\chi}}}$$

## The CR scattering rate

$$q_{e\tilde{\chi}} \sim \sigma_{e\tilde{\chi}} E_e \frac{d\phi}{dE_e} \sim \frac{a_R^2 e^2}{4\pi m_{\tilde{\chi}}^2} E_e \frac{d\phi}{dE_e}$$

## The ratio

$$\frac{q_{e\tilde{\chi}}}{q_{\tilde{\chi}\tilde{\chi}}} \sim 10^{-6} a_R^{-2} \left( \frac{E_e \frac{d\phi}{dE_e}}{\text{cm}^{-2} \text{s}^{-1}} \right) \left( \frac{m_{\tilde{\chi}}}{\text{GeV}} \right)$$

# Sensitivity e-ASTROGAM

M. Cermeño

Evidence for  
DM and its  
detection

Circular  
polarisation of  
photons from  
BSM  
interactions

Circular  
polarised  
signals from  
the GC  
(this work)

Conclusions

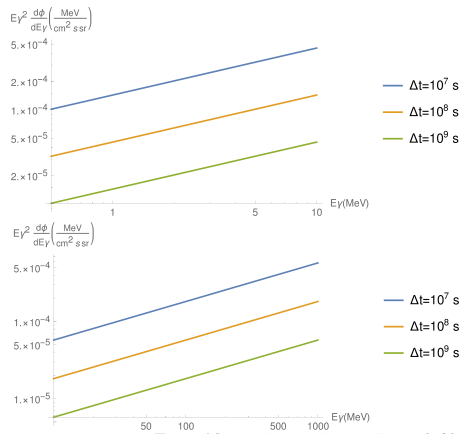
$$\epsilon = 0.013, A_{\text{eff}} = 50 - 560 \text{ cm}^2, E_\gamma = 0.3 - 10 \text{ MeV}$$

$$\epsilon = 0.3, A_{\text{eff}} = 215 - 1810 \text{ cm}^2, E_\gamma = 10 - 3000 \text{ MeV}$$

$$\frac{N_{\text{signal}}}{\sqrt{N_{\text{back}}}} \sim 3$$

$$\frac{\frac{d\Phi_{e\chi}}{dE_\gamma}}{\sqrt{\frac{d\Phi_{\text{back}}}{dE_\gamma}}} \sqrt{2\epsilon E_{\gamma,\text{peak}} \Delta\Omega A_{\text{eff}} \Delta t} = 3$$

$$E_\gamma^2 \frac{d\phi_{\text{back}}}{dE_\gamma} \sim 10^{-2} \text{ MeV cm}^{-2} \text{ s}^{-1} \text{ sr}^{-1}$$



# Sensitivity Fermi-LAT

M. Cermeño

Evidence for  
DM and its  
detection

Circular  
polarisation of  
photons from  
BSM  
interactions

Circular  
polarised  
signals from  
the GC  
(this work)

Conclusions

$$\epsilon \sim 0.1, A_{\text{eff}} \sim 10^4 \text{ cm}^2, E_\gamma \sim 1 \text{ GeV}$$

$$\frac{N_{\text{signal}}}{\sqrt{N_{\text{back}}}} \sim 3 \Rightarrow \frac{\frac{d\Phi_{e\chi}}{dE_\gamma}}{\sqrt{\frac{d\Phi_{\text{back}}}{dE_\gamma}}} \sqrt{2\epsilon E_{\gamma, \text{peak}} \Delta\Omega A_{\text{eff}} \Delta t} = 3$$

$$E_\gamma^2 \frac{d\phi_{\text{back}}}{dE_\gamma} \sim 10^{-2} \text{ MeV cm}^{-2} \text{ s}^{-1} \text{ sr}^{-1}$$

